

^{17}F breakup reactions: A touchstone for indirect measurements

C. Sfienti^{1,2}, G. Raciti[†], P. Capel^{3,4}, D. Baye⁴, M. De Napoli⁵,
F. Giacoppo^{5,6}, E. Rapisarda^{2,7}, G. Cardella², P. Descouvemont⁴,
C. Mazzocchi⁸ and J.-M. Sparenberg⁴.

¹ Dipartimento di Fisica e Astronomia, Università di Catania, I-95123, Catania, Italy.

² INFN-Sezione di Catania, I-95123, Catania, Italy.

³ National Superconducting Cyclotron Laboratory, MSU, East Lansing, MI 48824-1321, USA.

⁴ Physique Nucléaire et Physique Quantique (CP 229) ULB, B-1050 Brussels, Belgium.

⁵ INFN-Laboratori Nazionali del Sud, I-95123 Catania, Italy.

⁶ Dipartimento di Fisica, Università di Messina, I-98166 Messina, Italy.

⁷ Centro Siciliano di Fisica Nucleare e Struttura della Materia, I-95125 Catania, Italy.

⁸ INFN-Sezione di Milano and Università di Milano, I-20133, Milano Italy.

E-mail: Concettina.Sfienti@ct.infn.it

Abstract. Dissociation has become an essential tool in several domains of nuclear physics. It provides useful information about the structure of halo nuclei, and Coulomb breakup can be used as an indirect method to measure radiative-capture cross sections at stellar energies. Though simple it may seem, this indirect technique relies on peculiar assumptions. Recent theoretical analyses of the Coulomb breakup of ^8B have shown that these assumptions are not all satisfied.

Whereas many experimental investigations on such a phenomenon have been conducted on ^8B , the case of ^{17}F has been poorly addressed up to now. An exclusive study of ^{17}F breakup reactions has thus been performed at the FRIBs facility of the Laboratori Nazionali del Sud, Catania (Italy). The experimental setup and the detector systems allowed the measurement, event-by-event, of the X-Y coordinates of the interaction point on the target as well as the momenta and angles of all outgoing decay particles with a geometrical efficiency of 72% and a resolution of approximately 300 keV.

The first results and preliminary model comparison are reported.

1. Introduction

Dissociation of the atomic nucleus using energetic beams is nowadays an essential tool in several domains of nuclear physics. It is one of the few methods used to study the structure of nuclei far from stability, like halo nuclei [1]. It has also been proposed as an indirect technique to measure radiative-capture cross sections at stellar energies [2, 3], e.g., $^7\text{Be}(p, \gamma)^8\text{B}$. At these energies, the Coulomb barrier between the interacting nuclei hinders the capture, leading to so tiny cross sections that they cannot be measured in laboratories. Usually low-energy measurements are extrapolated down to the energy of the Gamow peak through reaction models. Unfortunately, this method is not free from biases. This has led to the search for indirect techniques like the Coulomb breakup. In that technique, the final nucleus synthesized in the radiative capture (^8B in the aforementioned example) is broken up into the initial nuclei (^7Be and p in the example)

by interaction with a heavy target. This reaction, being Coulomb dominated, may be seen as due to the exchange of virtual photons between the projectile and the target, and hence as the time-reversed reaction of the radiative capture. The basic idea of the Coulomb-breakup technique is thus to extract the radiative-capture cross section from the Coulomb breakup one via a detailed balance [3]. However, this can be done only under a few assumptions. First, the reaction must be purely Coulomb, i.e. the nuclear interaction between the projectile and the target must be negligible. Second, the radiative capture being dominated by E1 transitions at stellar energies, the influence of higher multipoles of the Coulomb interaction in the breakup process must be negligible. Finally, the direct link between the Coulomb-breakup cross section and the radiative capture one can only be made at the first order of the perturbation theory [4]. The dissociation must thus occur in one step from the bound state to the continuum, i.e. higher-order effects like couplings inside the continuum must be negligible.

Several Coulomb-breakup experiments of ${}^8\text{B}$ have been performed to extract the cross section of the reaction ${}^7\text{Be}(p, \gamma){}^8\text{B}$, which is a significant input for the study of solar-neutrino oscillations [5, 6]. Unfortunately, theoretical analyses suggest that E2 transitions [7, 8] and higher-order effects [7, 8, 9, 10] are not negligible. To assess the accuracy of the Coulomb-breakup technique, it is necessary to compare the cross section measured directly with the prediction obtained from a Coulomb-breakup measurement. Though extensively studied [5, 6, 7, 8], ${}^8\text{B}$ is not the best test case for this comparison. The direct measurements, being scattered over a wide range of values, are too discrepant for such a comparison. Moreover, the structure of ${}^8\text{B}$ is rather complicated and not well described as a proton loosely-bound to a structureless ${}^7\text{Be}$, as assumed in most of the reaction models. On the contrary, the ${}^{17}\text{F}$ case is well suited for such a study [3]: the direct radiative capture ${}^{16}\text{O}(p, \gamma){}^{17}\text{F}$ has been precisely measured down to 200 keV [11]. The nucleus ${}^{17}\text{F}$, being just one proton away from the doubly magic ${}^{16}\text{O}$, is well described as an ${}^{16}\text{O}$ core to which a proton is loosely bound [12]. Moreover, there is no resonance in the low-energy spectrum of ${}^{17}\text{F}$ that could influence the radiative-capture process at stellar energies. The only missing ingredient for this analysis is the Coulomb-breakup cross section, which is the aim of the Flubber experiment.

2. The FLUBBER Experiment

The ${}^{17}\text{F}$ beam has been produced at the in-Flight Radioactive Ion Beams (FRIBs) facility of the INFN-Laboratori Nazionali del Sud [13, 14]. At LNS a Superconducting Cyclotron delivers monoenergetic ion beams at incident energies ranging from 20 A MeV for the heaviest ions (like ${}^{238}\text{U}^{38+}$), up to 80 A MeV for protons and fully stripped light-ions. This energy range of primary beams allows the production of RIBs by projectile fragmentation reactions. In particular the extraction line of the cyclotron was already configured as a fragment separator. It consists of two dipole magnets and a series of quadrupoles. An energy degrader can be set at the dispersive focal plane between the two dipoles. The system allows the transmission of the produced fragments in a $B\rho$ range of about $\approx 1\%$ (with respect to the chosen $B\rho$ setting) and, therefore, a large number of radioactive isotopes will emerge at the final focus. Their identification is performed, on an event-by-event basis, through the *tagging technique*: it combines measurements of time-of-flight through the spectrometer, position tracking and energy loss, allowing the assignment (tag) of charge, mass, position and incident energy to each ion. The tagging detector must, obviously, not stop the incoming ions and should modify as little as possible their characteristics. Therefore, we applied the ΔE -ToF method to identify each incident fragment using the ΔE signal from a silicon detector and the time of flight measured from the same signal generated by the silicon detector with respect to the radiofrequency signal supplied by the accelerator (left plot of figure 1).

For our study a primary beam of ${}^{20}\text{Ne}$ was accelerated at an energy of 45 A MeV. In order to optimize the RIBs production, a ${}^9\text{Be}$ 500 μm thick production-target was used. The average primary beam current was about 350 enA. The beam was stopped at the injection of the cyclotron

during the dead time of the data acquisition system, in order to reduce the current at the cyclotron deflectors, the induced radioactivity on the beam lines and the radiation damage on the tagging detector. The mean beam intensity was then reduced down to about 170 enA, because bursts of 350 enA were sent 50% of the time. We obtained a total of 60 kHz of secondary beam on the tagging detector: 3 kHz of this mixture was ^{17}F with an incident energy of about 35 AMeV (right plot of figure 1). The tagging detector (a 24×24 X-Y Double Sided Silicon Strip Detector -DSSD- 2.5×2.5^2 cm of active area) was located in front of a three-position target holder containing an empty frame, a ^{nat}Pb 200 μm and a ^{12}C 350 μm thick targets to study both Coulomb- and nuclear-induced reactions.

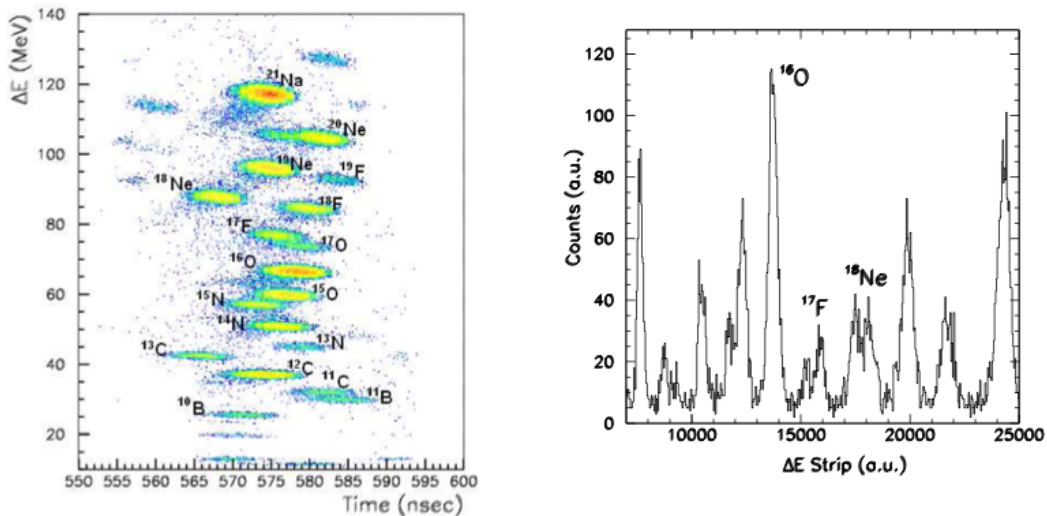


Figure 1. Left: ΔE -ToF identification from the Si-Strip detector. Right: Particle IDentification Spectrum on the Si-Strip detector.

The detection setup, placed at about 60 cm from the interaction target, consists of two Si-CsI hodoscopes, that cover the angular range between $\theta_{\text{lab}} = 0^\circ$ and 21.5° with high granularity and excellent isotopic resolution. The first is composed by 81 two-fold telescopes (300 μm Si detector $1 \times 1 \text{ cm}^2$ of active area followed by a 10 cm long CsI(Tl)) covering the forward angular range $\theta_{\text{lab}} < 5^\circ$. The second consists of 89 three-fold telescopes (50 + 300 μm Si detectors $3 \times 3 \text{ cm}^2$ active area followed by a 6 cm long CsI(Tl)) covering the angular range between $\theta_{\text{lab}} = 5^\circ$ and 21.5° . This experimental setup has already been used in the study of diproton decay of ^{18}Ne [15]. It allows the measurement, event-by-event, of the transverse coordinates of the interaction point on the target as well as of the momenta and angles of all outgoing decay particles in a solid angle of 0.34 sr around the beam direction with a geometrical efficiency of 72%. This set-up is thus well optimized for the measurement of the ^{17}F excitation energy as well as the individual and relative momenta, energies and angles of the two detected fragments (^{16}O and proton), with a resolution of approximately 300 keV.

3. Theoretical predictions

The model considered is the Dynamical Eikonal Approximation (DEA) [16]. It corresponds to the eikonal approximation without the adiabatic approximation, which is usually subsequently made. The DEA therefore takes full account of the internal dynamics of the projectile, which enables us to describe both nuclear- and Coulomb-dominated reactions within one model. It has successfully described various reactions involving loosely-bound nuclei [16, 8]. In particular

the DEA could explain most of the features of the observables measured in Coulomb-breakup experiments of ^8B at intermediate energies [8]. This makes thus the DEA the ideal theoretical model to analyse the Flubber experiment.

The ^{17}F is described as a proton loosely bound to an ^{16}O core, assumed to be in its 0^+ ground state. The interaction between these two clusters is described by a Woods-Saxon potential fitted to reproduce the energy and quantum numbers of the two bound states of ^{17}F [12]. The $5/2^+$ ground state at 600 keV below the one-proton separation threshold is modelled as a $0d5/2$ state, while the $1/2^+$ excited state, bound by a mere 100 keV, is described as a $1s1/2$ state. The potential also reproduces the $3/2^+$ resonance at 4.4 MeV above the one-proton separation threshold in the $d3/2$ partial wave. The interaction between the two components of the projectile with the target are simulated by optical potentials chosen in the literature. For the p-target potential, the global parametrisation of Koning and Delaroche has been considered [17]. The ^{16}O -target interaction is simulated by the optical potentials developed by Roussel-Chomaz *et al* [18] to describe the elastic scattering of ^{16}O on various targets at 94 A MeV. The energy dependence in the latter case is neglected.

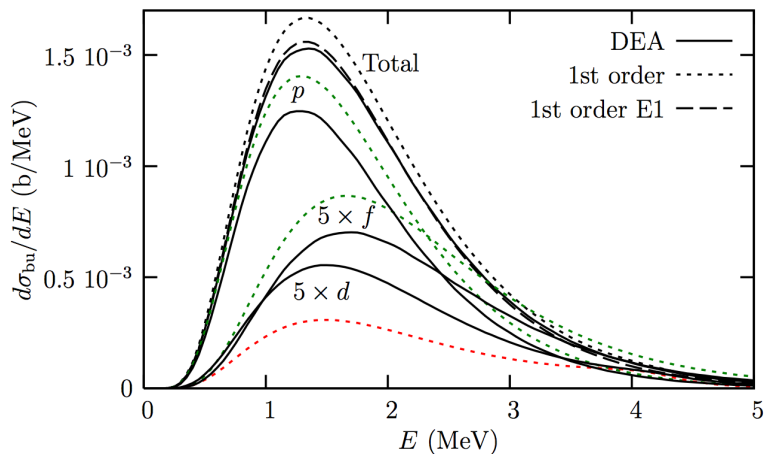


Figure 2. Theoretical prediction of the breakup cross section of ^{17}F on lead at 40 A MeV limited to forward angles as a function of the relative ^{16}O -p energy after dissociation.

Figure 2 displays the theoretical prediction for the breakup cross section of ^{17}F on lead at 40 A MeV as a function of the relative energy E between ^{16}O and the proton after dissociation. A forward-angle selection is simulated by an impact parameter cutoff at $b_{\min} = 40$ fm. The contribution of the major partial waves are shown as well. The full lines correspond to the DEA calculation, while the dotted lines are the results obtained at the first-order of the perturbation theory [4]. As can be seen, the reaction is dominated by E1 transitions from the d ground state to the p and f continua. However, we note a non-negligible d contribution that can be explained at the first-order only by E2 transitions. We also observe that the first-order calculation differs from the dynamical one: The former indeed overestimates the latter. However, this overestimation is not observed in all partial waves. Indeed, while both the p and f contributions are overestimated at the first-order, the d wave is underestimated. In agreement with a previous study [10], we interpret this as a signature of higher-order effects. In these higher-order effects, the p and f continua, directly populated from the ground state by E1 transitions, are depopulated towards the d partial waves through E1 couplings inside the continuum. This increases the population of the d waves in the continuum already fed by direct E2 transitions from the bound state. Curiously the dynamical calculation is rather well simulated by a first-order calculation including only E1 transitions (dashed line in figure 2), as already noted in an analysis of ^8B breakup [10].

4. Preliminary Results and model comparison

The ^{17}F was selected among the different isotopes of the secondary beam by gating on the ΔE -ToF plot provided by the DSSD detector (Fig 1). For this preliminary stage of the analysis the conditions to be satisfied by the event are:

- (i) A ^{17}F detected in one front strip;
- (ii) No other projectiles detected in the same event;
- (iii) Only one backward strip fired or two adjacent backwards strips fired, if the sum of the measured energies is almost equal to the energy measured by the front strip.

To study the $^{17}\text{F} \rightarrow ^{16}\text{O} + \text{p}$ decay channel, we considered only the tagging gated events in which one ^{16}O and one proton have been detected by the hodoscopes ($\mathcal{M} = 2$). Moreover, in order to select very peripheral reactions, only events in which the residue was detected at small emission angles, and both the particle and residue had velocities close to that of the incident beam were chosen. Even though this stringent set of cuts on the data considerably reduced the statistics, it produces an ensemble of *gold-plated* breakup events.

The $^{17}\text{F} \rightarrow ^{16}\text{O} + \text{p}$ channel, being a two-body decay, can be kinematically identified and reconstructed once the energies and emission angles (θ and ϕ) of the two particles are measured. By a complete kinematical reconstruction from the velocities and angles of the decay products, the CM velocity, the excitation-energy spectrum of the projectile and the relative momentum of the decay products can be estimated.

Before comparing the experimental data with the model, its theoretical predictions need to be filtered, taking into account the efficiency and the energy resolution of the experimental setup. In order to simulate the experimental conditions a Monte Carlo simulation has been developed. In the simulation the geometry of the two hodoscopes is included, as well as the energy thresholds and the energy resolution of each telescope. The introduction of the experimental filter does not substantially change the shape of the relative energy distribution (figure 3 full line -left plot). Despite the low statistics the experimental spectrum nicely confirms the theoretical predictions.

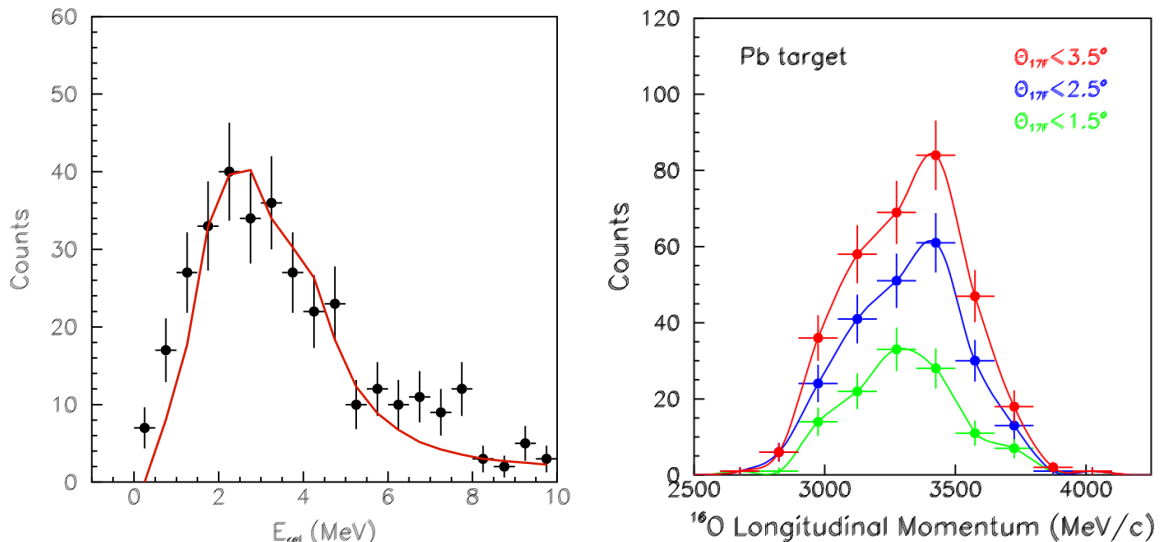


Figure 3. Left: Experimental relative energy distribution (black dots) compared to DEA predictions filtered for the experimental conditions (red line). Right: Measured longitudinal momentum distributions of ^{16}O fragments from the Coulomb dissociation of 40 MeV/nucleon ^{17}F for several reconstructed maximum ^{17}F scattering angle cuts (solid line are only to guide the eye).

This preliminary comparison suggests that both E2 contribution and higher orders take place during the reaction. To further investigate these contributions the longitudinal momentum distributions of ^{16}O have been extracted. In particular different selection cuts have been applied to the data, gating on the ^{17}F reconstructed maximum scattering angle (figure 3 -right plot). The shape of the distribution is quite asymmetric especially for larger scattering angle. Indeed, as already pointed out in [6], the longitudinal momentum distributions reveal E2 strength in the Coulomb breakup in the form of an asymmetry produced by E1-E2 interference. Similar signatures have been obtained from inspection of the proton transverse momenta. Clearly in both cases a more quantitative comparison between the measured observables and the theoretical predictions is mandatory to deduce the effective role played by the E2 strength and the higher-order effects in the Coulomb breakup.

5. Conclusion

The Flubber experiment has been performed with the aim of testing the accuracy of the Coulomb-breakup indirect technique used to infer radiative-capture cross sections at low energies. This technique has been used in the $^7\text{Be}(p, \gamma)^8\text{B}$ case [5, 6], but has never been tested. By measuring the breakup of ^{17}F into $^{16}\text{O}+p$, and comparing the inferred cross section for $^{16}\text{O}(p, \gamma)^{17}\text{F}$ to direct precise measurements [11], we hope to evaluate the influence of E2 transitions and higher-order effects, that are theoretically predicted to be significant in Coulomb-breakup reactions [9, 10].

The measured relative energy distribution nicely agrees with the model prediction, indicating the occurrence of higher-order effects in breakup reactions. All of the measured longitudinal and transverse momentum distributions share a common feature: an asymmetry attributed to interference between E1 and E2 transition amplitudes in the Coulomb breakup.

Acknowledgments

The present project is partly funded within the IXth programme of scientific cooperation between the French community of Belgium and Italy.

References

- [1] Tanihata I, 1996 *J. Phys. G* **22** 157
- [2] Baur G, Bertulani C.A, and Rebel H, 1986 *Nucl. Phys. A* **458** 188
- [3] Baur G and Rebel H, 1996 *Annu. Rev. Nucl. Part. Sci.* **46** 321
- [4] Alder K and Winther A, *Electromagnetic Excitation* (North-Holland, Amsterdam, 1975)
- [5] Motobayashi T *et al.* 1994 *Phys. Rev. Lett.* **73** 2680
- [6] Davids B, Austin S.M, Bazin D, Esbensen H, Sherrill B.M, Thompson I.J, Tostevin J.A, 2001 *Phys. Rev. C* **63** 065806
- [7] Esbensen H and Bertsch G.F, 1996 *Nucl. Phys. A* **600** 37
- [8] Goldstein G, Capel P, and Baye D, 2007 *Phys. Rev. C* **76** 024608
- [9] Esbensen H, Bertsch G.F, and Snover K.A, 2005 *Phys. Rev. Lett.* **94** 042502
- [10] Capel P and Baye D, 2005 *Phys. Rev. C* **71** 044609
- [11] Morlock R, Kunz R, Mayer A, Jaeger M, Müller A, Hammer J.W, Mohr P, Oberhummer H, Staudt G, Kölle V, 1997 *Phys. Rev. Lett.* **79** 3837
- [12] Sparenberg J.-M, Baye D, and Imanishi B, 2000 *Phys. Rev. C* **61** 054610
- [13] Raciti G, Rapisarda E, De Napoli M, Amorini F, Calabretta L, Cardella G, Cosentino G, Sfienti C, and Shchepunov V, 2008 *Nucl. Instrum. Methods B* **266** 4632
- [14] Rapisarda E, Raciti G, De Napoli M, Calabretta L, Cardella G and Sfienti C, this conference proceedings
- [15] Raciti G, Cardella G, De Napoli M, Rapisarda E, Amorini F, and Sfienti C, 2008 *Phys. Rev. Lett.* **100** 192503
- [16] Baye D, Capel P, and Goldstein G, 2005 *Phys. Rev. Lett.* **95** 082502
- [17] Koning A.J and Delaroche J.P, 2003 *Nucl. Phys. A* **713** 231
- [18] Roussel-Chomaz P, Alamanos N, Auger F, Barrette J, Berthier B, Fernandez B, Papineau L, Doubre H, Mittag W, 1988 *Nucl. Phys. A* **477** 345